

# Decoherence of Rabi oscillations in a single quantum dot

J. M. Villas-Bôas,<sup>1,2</sup> Sergio E. Ulloa,<sup>1</sup> and A. O. Govorov<sup>1</sup>

<sup>1</sup>*Department of Physics and Astronomy, and Nanoscale and Quantum Phenomena Institute, Ohio University, Athens, Ohio 45701-2979*

<sup>2</sup>*Departamento de Física, Universidade Federal de São Carlos, 13565-905, São Carlos, São Paulo, Brazil*

We develop a realistic model of Rabi oscillations in a quantum-dot photodiode. Based in a multi-exciton density matrix formulation we show that for short pulses the two-level models fails and higher levels should be taken into account. This affects some of the experimental conclusions, such as the inferred efficiency of the state rotation (population inversion) and the deduced value of the dipole interaction. We also show that the damping observed cannot be explained using *constant* rates with fixed pulse duration. We demonstrate that the damping observed is in fact induced by an off-resonant excitation to or from the continuum of wetting layer states. Our model describes the nonlinear decoherence behavior observed in recent experiments.

Coherent manipulation of a quantum state is one of the tasks required in quantum computation and information processing. Semiconductor quantum dots (QDs) have been shown to be excellent candidates for the physical implementation of these objectives. Rabi oscillations – temporal coherent oscillations of the population and its inversion in a two-level system driven by a strong resonant field – have been successfully demonstrated by different groups using excitons in single QDs with different clever probing techniques,<sup>1,2,3,4,5,6,7,8</sup> as well as utilizing the biexciton population.<sup>9</sup> Zrenner *et al.*<sup>4</sup> have developed a single self-assembled QD photodiode in which the population inversion is probed by the photocurrent signal induced by a strong and carefully tuned optical pulse. In their device the pulse generates an electron-hole pair in the QD and with the help of an external gate voltage, the electron and hole tunnel out into nearby contacts. This process generates a photocurrent signal that is a weakly disturbing probe of the coherent state of the system. Their results show Rabi oscillations that are damped with increasing area of the pulse for a fixed pulse duration. However, the mechanisms that produce this decoherence were unclear.

We present a study of the dynamics of a single self-assembled quantum dot photodiode in the presence of an optical pulse. The electron and hole tunneling processes are introduced via a microscopic model of the structure which also includes the electron-hole interaction. The dynamics is described using a density matrix approach that incorporates dipole coupling to multi-exciton states and off-resonant excitation to states in the wetting layer (WL). Our model shows that for short pulses (of the order of a few ps, as used in experiments<sup>4</sup>) the two level system approximation fails for a  $\pi$ -pulse (the pulse necessary to invert the exciton population) and the biexciton state plays an important role in the dynamics. This results in a frequency shift of the measured photocurrent oscillations, which can significantly affect the experimentally deduced value of the transition dipole moment. The efficiency estimate of the state rotation (population inversion) for a  $\pi$ -pulse is also affected as the biexciton contributes to the photo-signal. We demonstrate that

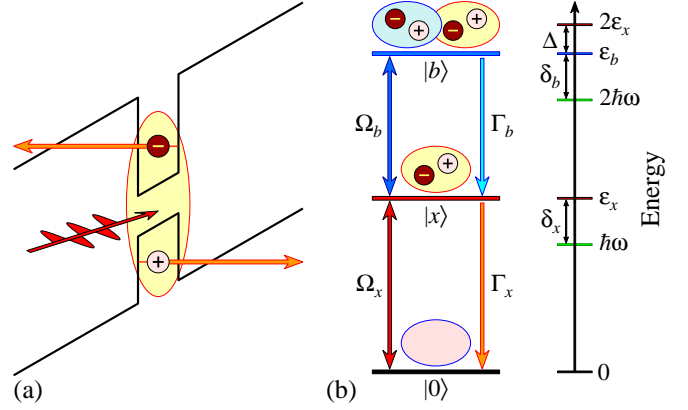


FIG. 1: Schematic band structure and level configuration of QD photodiode. (a) An electromagnetic pulse creates an exciton in the dot, and an applied gate voltage forces the electron and hole to tunnel out, generating the photocurrent signal. (b) Schematic representation of processes and levels involved in this system:  $|x\rangle$  and  $|b\rangle$  are exciton and biexciton states.

longer pulses minimize the biexciton contribution. Most importantly, we find that inclusion of excitations to WL states is essential to understand the decoherence observed in experiments. The damping due to coupling with the WL not only explains the observed shape of Rabi oscillations, but also gives a description of the background signal observed in Rabi-photodiodes.<sup>10</sup> Although we focus on the QD photodiode,<sup>4</sup> our model is also relevant for experiments on Rabi oscillations with optical readout.<sup>8</sup>

In Fig. 1 we show the system and level configuration taken into account by our model Hamiltonian which can be written as<sup>11</sup>

$$H_0 = \delta_x |x\rangle\langle x| + \delta_b |b\rangle\langle b| - \frac{1}{2} \left[ \Omega_x(t) |0\rangle\langle x| + \Omega_b(t) |x\rangle\langle b| + h.c. \right]. \quad (1)$$

Here,  $\delta_x = \varepsilon_x - \hbar\omega$  accounts for the detuning of the exciton with the laser energy  $\hbar\omega$ ,  $\delta_b = \varepsilon_b - 2\hbar\omega$  is the two photon biexciton detuning,  $\Omega_x(t) = \langle 0 | \vec{\mu} \cdot \vec{E}(t) | x \rangle / \hbar$ ,  $\Omega_b(t) = \langle x | \vec{\mu} \cdot \vec{E}(t) | b \rangle / \hbar$ , where the electric dipole moment  $\vec{\mu}$  describes the coupling of the excitonic transition to the

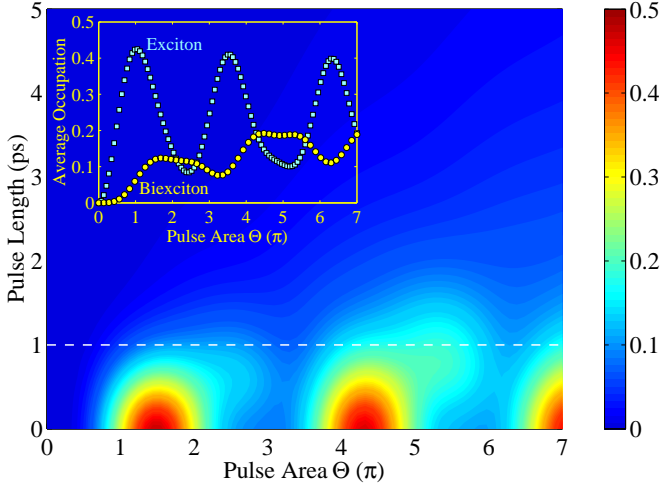


FIG. 2: Contour plot of the biexciton average occupation as function of pulse duration  $t_p$  and pulse area  $\Theta$ . Notice long pulses do not produce biexciton population. Inset compares exciton and biexciton contribution for a 1 ps pulse.

radiation field, and  $\vec{E}(t)$  is the pulse amplitude which we assume to have a Gaussian shape, with full width at half-maximum (FWHM)  $t_p$  (pulse length).

For a strong pulse resonant with the exciton energy ( $\delta_x = 0$ ), the biexciton binding energy  $\Delta = 3$  meV is relatively small and, as can be seen in Fig. 2, cannot be neglected in the dynamical description of the system. There we show the average occupation of the biexciton state as a function of the pulse length  $t_p$  and pulse area  $\Theta = \int_{-\infty}^{\infty} \Omega(t) dt$ , assuming that the biexciton has the same dipole moment of the exciton transition<sup>12</sup> [ $\Omega_b(t) = \Omega_x(t) = \Omega(t)$ ] and not including decay or dephasing. We show below that even after inclusion of these effects the biexciton population is important for short pulses.

The dynamics of the reduced system is computed using a master equation in the Lindblad form<sup>13</sup>

$$\frac{d\rho}{dt} = -\frac{i}{\hbar}[H_0, \rho] + L(\rho), \quad (2)$$

where the first term on the right yields the unitary evolution of the quantum system and  $L(\rho)$  is the dissipative part of the evolution assuming the Markovian approximation. We use  $\Gamma_i$  to describe all population decay rates of the level  $i$ , which we assume to have two different sources, one due to the spontaneous decay  $\Gamma_i^{\text{rec}}$  given by the recombination rate (for the exciton state the spontaneous decay time is known to be  $\tau_{\text{rec}} = 1/\Gamma_x^{\text{rec}} \simeq 1$  ns for this kind of QD) and other  $\Gamma_i^{\text{tun}}$  which results when the particles (making the exciton or biexciton) leave the system by tunneling, so that  $\Gamma_i = \Gamma_i^{\text{tun}} + \Gamma_i^{\text{rec}}$ .

We can estimate the tunneling rate  $\Gamma_s^{\text{tun}}$  for a single particle  $s$  (electron or hole) using the tunneling Hamiltonian.<sup>14,15</sup> The probability of 0D to 3D tunneling for a single particle is<sup>14</sup>  $\Gamma_s^{\text{tun}} = \frac{2\pi}{\hbar} \sum_{\alpha} |\langle \Psi_s | V_{\text{Dot}} | \Psi_{\alpha} \rangle|^2 \delta(E_s - E_{\alpha})$ , where  $\Psi_s$  and  $E_s$  is the single particle wave function (for electron or hole)

localized in the QD and its respective energy, while  $\Psi_{\alpha}$  and  $E_{\alpha}$  are correspondingly in the contacts. In  $\Psi_{\alpha}$  we use plane waves for the in-plane motion, and the  $z$ -component was calculated using the linear potential from the applied gate voltage and an exponential decay function in the barrier region.<sup>16</sup>  $\Psi_s$  is strongly localized in the quantum dot, and it is modelled as  $\Psi_s(r, z) = \frac{1}{\sqrt{\pi} l_s} \exp(-\frac{r^2}{2l_0^2}) \chi(z)$ , the product of a ground state harmonic-oscillator function which describes the lateral motion in a quantum dot, and  $\chi(z)$ , the wave function of a square well potential. We obtain

$$\Gamma_s^{\text{tun}} = \left( \frac{4V_s}{\pi\hbar} \right)^2 \sqrt{\frac{L^2 m_s^*}{2|E_s|}} \exp\left( -\frac{4}{3} \frac{\sqrt{2m_s^*}}{\hbar e F} |E_s|^{\frac{3}{2}} \right), \quad (3)$$

where  $m_s^*$  is the effective mass of the particle  $s$  in the dot,  $L$  and  $V_s$  are the width and depth of the corresponding square well, and  $F$  is the electric field provided by the gate voltage. This is similar to the WKB tunneling but with well-characterized energy dependent prefactor.

One can consider as a good first approximation that the electron-hole interaction produces a shift (the exciton binding energy) in the single particle energy level  $E_s$  in the quantum dot, and use Eq. 3 to obtain the rates with and without electron-hole interaction. Note that this estimate of the carrier tunneling time  $\tau_s^{\text{tun}} = 1/\Gamma_s^{\text{tun}}$  cannot be directly compared with the experimental linewidth of the photocurrent peak since that reflects the time for *both* particles to tunnel out of the system (even if dominated by the faster rate). Using parameters from Ref. [17] and the assumption that  $V_e \simeq 3V_h$  (where  $V_e$  ( $V_h$ ) is the electron (hole) depth of the square well profile), we obtain that the tunneling times for electron or hole are similar when there is electron-hole interaction (this of course depends on QD parameters). After one of the particle tunnels, the remaining particle tunnels out faster, as it no longer experiences the electron-hole interaction. The rates we consider here,  $\Gamma_x^{\text{tun}}$  for the exciton and  $\Gamma_b^{\text{tun}}$  for the biexciton, are the rates for all particles (electrons and holes) to leave the system, and they are obtained by solving a separate density matrix equation including the different tunneling rates for individual single-particle states. For the exciton state for instance, we solve a four dimensional density matrix which includes the vacuum, exciton, electron (when the hole leaves the system first) and hole states (when the electron leaves the system first). Solving this density matrix one can evaluate the equivalent rate for a two level system that reproduces the multipath process. We obtain  $\Gamma_x^{\text{tun}} = 1/\tau_x^{\text{tun}}$ , where  $\tau_x^{\text{tun}} \simeq 12$  ps is the time for both particles to leave the system by tunneling, and is consistent with the photocurrent signal linewidth ( $\simeq 10$  ps). We can consider this tunneling as a single process because the charged exciton, which could be created from a single particle state (after one particle leaves the QD), is  $\simeq 4.6$  meV out of resonance from the exciton state excitation for this kind of QD,<sup>17</sup> and cannot be created during the pulse duration which is much faster than the single particle tunneling time. A similar

description applies to the biexciton state. This allows us to write a simple equation for the photocurrent signal in terms of the exciton and biexciton contributions as we now describe.

As the photocurrent is a signal induced by the particles that tunnel out, when the next pulse arrives the system is already in the vacuum state  $|0\rangle$  (meaning that they are different processes that account for a statistical average), we can write the expression for the photocurrent as

$$I_{PC} = fq \left[ \Gamma_b^{\text{tun}} \int_{-\infty}^{\infty} \rho_{bb}(t) dt + \Gamma_x^{\text{tun}} \int_{-\infty}^{\infty} \rho_{xx}(t) dt \right], \quad (4)$$

where  $f$  is the repetition frequency of the pulse sequence (we use  $f = 82$  MHz as in Zrenner's experiment<sup>4</sup>) and  $q$  is the electronic charge. One can also write this as

$$I_{PC} = fq \left[ \Gamma_b^{\text{tun}} \int_{-\infty}^{\tau} \rho_{bb}(t) dt + \Gamma_x^{\text{tun}} \int_{-\infty}^{\tau} \rho_{xx}(t) dt + \frac{\Gamma_b^{\text{tun}}}{\Gamma_b} \rho_{bb}(\tau) + \frac{\Gamma_x^{\text{tun}}}{\Gamma_x} (\rho_{xx}(\tau) + \rho_{bb}(\tau)) \right], \quad (5)$$

where  $\tau$  is the time at end of the pulse. Notice that the result is not a simple summation of exciton and biexciton contributions, but it is rather a mixture. This is expected, as the biexciton occupation after the pulse eventually decays to the exciton state, and contributes to the exciton part of the photocurrent. It is important to point out that even if we ignore the biexciton contribution to Eq. 5, it still exhibits a term not considered before:<sup>4</sup> the contribution during the pulse given by the second integral in Eq. 5. This contribution can indeed be small depending on the tunneling time and/or pulse duration. However, it is not the case here, as shown in Fig. 3, where the different Eq. 5 contributions to the photocurrent are shown. Blue squares show the results without the contribution during the pulse (the second integral in Eq. 5) and neglecting the biexciton state in the entire simulation. The yellow circles show the same simulation but including the extra integral term. The difference between the two traces is noticeable and cannot be ignored. Including the biexciton in the simulation and using the full Eq. 5 results in a photocurrent trace that exhibits decay of the oscillations, but increases slightly with the pulse area, which is not consistent with experimental observations.

Experimental results exhibit a decay of the oscillation with increasing pulse area, which cannot be obtained from our model so far. Notice that any kind of additional *constant* decay or dephasing cannot explain the experimental trace either, since increasing the pulse area makes this quantity smaller compared with the pulse intensity, and the Rabi oscillations are enhanced overall. This behavior indicates the presence of other levels that contribute to decoherence in the system.<sup>20</sup> It has been recently demonstrated that the level continuum in the wetting layer (WL) plays an important role in the background absorption in self-assembled QDs at high energies.<sup>18</sup> We here include the dephasing produced

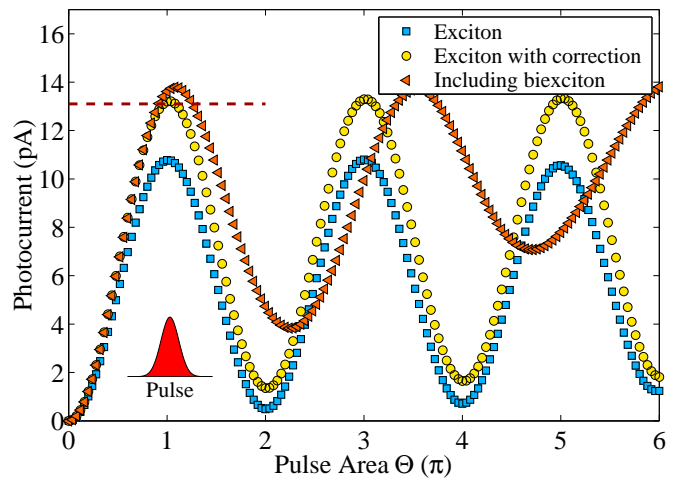


FIG. 3: Photocurrent signal as function of pulse area  $\Theta$  for 1 ps pulse showing different contributions of Eq. 5. Blue squares show results neglecting biexcitons and without the second integral in Eq. 5; yellow circles include the latter. Triangles show results including biexcitons and all terms in Eq. 5. Dashed line at  $I_{PC} = fq \simeq 13.1$  pA indicates optimum value for photocurrent if only exciton channel is considered.

by the WL continuum, which in essence is being populated non-resonantly by the light pulse and then contributes to the dephasing of all the low-energy excitations. It is possible to excite electrons from a bound state in the QD (valence band) to the continuum of the WL (conduction) and from the continuum (valence) to bound (conduction).<sup>18</sup> We can model the WL as a unique level detuned from the exciton states by  $\delta_w$ , and coherently connected to the ground state by a dipole interaction  $\Omega_w$ . This results in an additional term to the Hamiltonian  $H_0$  given by  $H_w = \delta_w |w\rangle\langle w| - \frac{1}{2} \Omega_w(t) |0\rangle\langle w| + h.c.$ . The electron or hole in this WL state will scatter quickly and leave behind the other localized single particle  $s$ . We describe this process by one decay rate  $\Gamma_w$ , which connects the WL states to  $s$ . This process is shown in Fig. 4(a) where it is represented by a one-direction arrow. Eventually the electron or hole in this  $s$  state will tunnel and the system will return to its ground state. This connection is modelled by  $\Gamma_s$ , and given by Eq. 3. Following the same analysis as for the biexciton, we would not expect to populate these levels for low intensity, since they are apparently far detuned from the laser energy. However, the WL level broadening allows this process to take place, resulting in these extra levels being populated with increasing pulse intensity, and a growing background signal in the photocurrent (as that subtracted in experiments). This is clearly shown in Fig. 4(b), where we compare the occupation of some states of the system, with  $\delta_w = 20$  meV,  $\Gamma_w = 40$  meV,  $\Omega_w = \Omega_x$ , and,  $\Gamma_s = \Gamma_s^{\text{tun}}$  given by Eq. 3. Figure 4(c) shows the resulting photocurrent obtained from Eq. 5, without the background contribution of the WL. The photocurrent exhibits a decay of the oscillation induced by the nonresonant excitation to the WL

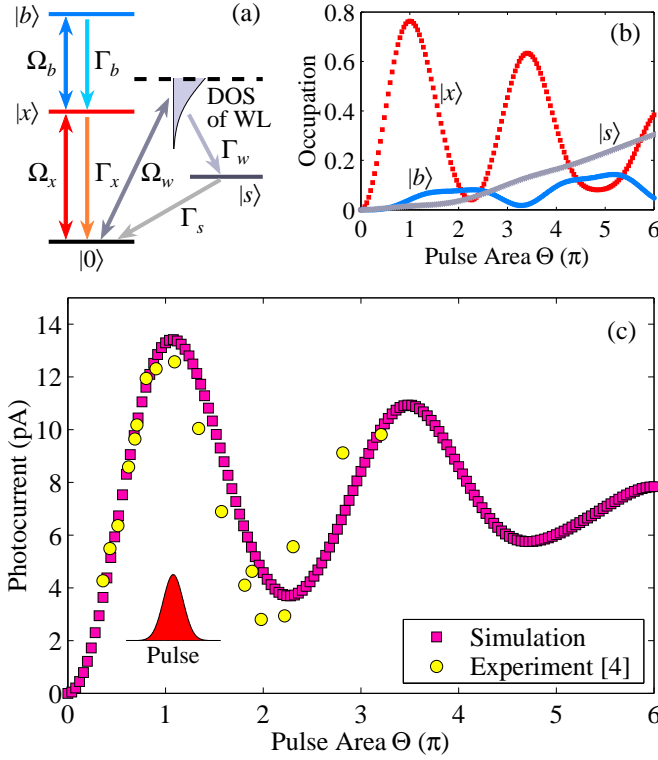


FIG. 4: (a) Level structure and couplings including nonresonant excitation to wetting layer WL. (b) Occupation probability of states considered in model as function of pulse area  $\Theta$ . (c) Photocurrent signal vs.  $\Theta$  for 1 ps pulse. Squares show results of our model and circles are experimental data from Ref. [4]. Notice this model reproduces experimental results.

and it fits quite well the experimental result (although no fine tuning of parameters has been done).<sup>4</sup>

We have described the WL by an additional level that is coherently excited out of resonance. In reality, the WL has a broad continuous distribution of levels resulting in an incoherent pump excitation, since we have a one-way excitation, as can be seen in Fig. 4(a,b) (the population

of state  $s$  only increases). Therefore, we can propose an equivalent model that involves a leakage rate  $\Gamma_{WL}$  connecting the ground state  $|0\rangle$  to the WL continuum  $\Gamma_{WL} = \frac{2\pi}{\hbar} \sum_{\nu} \left| \frac{1}{2} \langle \nu | \vec{\mu} \cdot \vec{E}(t) | 0 \rangle \right|^2 \delta(E_{\nu} - E_0 - \hbar\omega)$ , where the summation is over all  $\nu$  levels that compose the WL. This can be written as

$$\Gamma_{WL} = \frac{\pi}{2\hbar} \rho_{WL} \mu_w^2 E(t)^2, \quad (6)$$

where  $\rho_{WL}$  is the WL density of states, and  $\mu_w$  is the effective dipole moment connecting the WL continuum to the dot ground state. The master equation (2) with rate (6) gives quantitatively similar results to those shown in Fig. 4(c) if we use a density of states  $\rho_{WL} = \frac{1}{\pi} \frac{\Gamma_w/2}{\Gamma_w^2/4 + \delta_w^2}$ , where  $\delta_w$  is the WL detuning with the laser, and  $\Gamma_w$  is the broadening of the WL levels from our previous model. Notice that this channel naturally results in an intensity dependent decoherence, as that described recently.<sup>8,19</sup>

We have presented a realistic model to describe the Rabi oscillations observed in a single QD photodiode in the presence of pulsed light. Using a model that includes multi-exciton and WL states, a density matrix formalism shows that the two-level model breaks down and gives an imprecise interpretation of the results. Full inclusion of the biexciton allowed us to derive an expression for the photocurrent signal that corrects the simplest model used in the literature, and more precisely assesses the efficiency of the level rotation. Our study of the damping mechanisms makes us conclude that the only possibility to explain the damping with increasing pulse area (and fixed pulse duration) is an off-resonant excitation to a different level. This is identified most likely as the WL continuum of levels. This would also explain the background in the photocurrent signal observed in experiments.<sup>10</sup>

This work was partially supported by FAPESP, the US DOE grant no. DE-FG02-91ER45334, and the Indiana 21st Century Fund. We thank C.J. Villas-Bôas, N. Stuard, A. Muller, P. Bianucci, A.H. MacDonald, and L.E. Oliveira for helpful discussions.

- <sup>1</sup> T. H. Stievater *et al.*, Phys. Rev. Lett. **87**, 133603 (2001).
- <sup>2</sup> H. Kamada *et al.*, Phys. Rev. Lett. **87**, 246401 (2001).
- <sup>3</sup> H. Htoon *et al.*, Phys. Rev. Lett. **88**, 087401 (2002).
- <sup>4</sup> A. Zrenner *et al.*, Nature (London) **418**, 612 (2002).
- <sup>5</sup> P. Borri *et al.*, Phys. Rev. B **66**, 081306(R) (2002).
- <sup>6</sup> L. Besombes, J. J. Baumberg, and J. Motohisa, Phys. Rev. Lett. **90**, 257402 (2003).
- <sup>7</sup> A. Muller *et al.*, Appl. Phys. Lett. **84**, 981 (2004).
- <sup>8</sup> Q. Q. Wang *et al.*, cond-mat/0404465 (2004).
- <sup>9</sup> X. Li *et al.*, Science **301**, 809 (2003).
- <sup>10</sup> E. Beham *et al.*, Physica E **16**, 59 (2003).
- <sup>11</sup> J. M. Villas-Bôas, A. O. Govorov, Sergio E. Ulloa, Phys. Rev. B **69**, 125342 (2004).
- <sup>12</sup> G. Chen *et al.*, Phys. Rev. Lett. **88**, 117901 (2002).
- <sup>13</sup> G. Mahler and V. A. Weberruß, *Quantum Networks: Dynamics of Open Nanostructures* (Springer, Berlin, 1998).

- <sup>14</sup> R. J. Luyken *et al.*, Appl. Phys. Lett. **74**, 2486 (1999); A. O. Govorov and W. Hansen, Phys. Rev. B **58**, 12980 (1998).
- <sup>15</sup> J. Bardeen, Phys. Rev. Lett. **6**, 57 (1961).
- <sup>16</sup> L. D. Landau and E. M. Lifshitz, *Quantum Mechanics* (Pergamon, Oxford, 1975).
- <sup>17</sup> F. Findeis *et al.*, Phys. Rev. B **63**, 121309(R) (2001).
- <sup>18</sup> A. Vasanelli, R. Ferreira, and G. Bastard, Phys. Rev. Lett. **89**, 216804 (2002).
- <sup>19</sup> H. S. Brandi *et al.*, unpublished preprint.
- <sup>20</sup> Note that acoustic phonons can be another source of decoherence for Rabi oscillations. See J. Forstner *et al.*, Phys. Rev. Lett. **91**, 127401 (2003); V. M. Axt, P. Machnikowski, and T. Kuhn, cond-mat/0408322.